DMD Fast Forward. Published on May 22, 2017 as DOI: 10.1124/dmd.117.076307
This article has not been copyedited and formatted. The final version may differ from this version.

CRISPR/Cas9 genetic modification of *CYP3A5 *3* in HuH-7 human hepatocyte cell line leads to cell lines with increased midazolam and tacrolimus metabolism

Casey R. Dorr, Rory P. Remmel, Amutha Muthusamy, James Fisher, Branden Moriarity, Kazuto Yasuda , Baolin Wu, Weihua Guan, Erin Schuetz, William S. Oetting, Pamala A. Jacobson and Ajay K. Israni

Primary Laboratory of Origin:

Molecular Epidemiology Lab, Minneapolis Medical Research Foundation (CRD, AM, AKI), Minneapolis, MN.

DMD Fast Forward. Published on May 22, 2017 as DOI: 10.1124/dmd.117.076307
This article has not been copyedited and formatted. The final version may differ from this version.

Running Title:

CRISPR modification of *CYP3A5* in HuH-7 alters drug metabolism

Corresponding author:

Ajay K. Israni, M.D., M.S.

Hennepin County Medical Center,

Department of Medicine,

Nephrology Division,

701 Park Avenue,

Minneapolis, MN 55415-1829

612-873-6987

israni001@umn.edu

Number of text pages: 33

Number of tables: 1

Number of figures: 9

Number of references: 37

Number of words in the Abstract: 150

Number of words in the Introduction: 887

Number of words in the Discussion: 1160

DMD Fast Forward. Published on May 22, 2017 as DOI: 10.1124/dmd.117.076307
This article has not been copyedited and formatted. The final version may differ from this version.

Abbreviations:

CRISPR = Clustered regularly interspaced short palindromic repeats

CYP = Cytochrome P450

Tac = tacrolimus

MDZ = midazolam

1-OH MDZ = 1-hydroxy midazolam

4-OH MDZ = 4- hydroxyl midazolam

AA = African American

sd = single deletion

dd = double deletion

pm = point mutation

PAM = Protospacer adjacent motif

SNP = single nucleotide polymorphisms

HDR = Homology directed repair

NHEJ = non-homologous end joining

bp = base pairs

PCR = polymerase chain reaction

qRT-PCR = quantitative reverse transcriptase polymerase chain reaction

Abstract:

CRISPR/Cas9 engineering of the *CYP3A5 *3* locus (rs776746) in human liver cell line HuH-7 (*CYP3A5 *3/*3*) led to three *CYP3A5 *1* cell lines by deletion of the exon 3B splice junction or point mutation. Cell lines *CYP3A5 *1/*3 sd* (single deletion), *CYP3A5 *1/*1* dd (double deletion) or *CYP3A5 *1/*3* pm (point mutation) expressed the *CYP3A5 *1* mRNA, had elevated *CYP3A5* mRNA ($p<0.0005$ for all engineered cell lines) and protein expression compared with HuH-7. In metabolism assays, HuH-7 had less tacrolimus (Tac) (all p-values < 0.05) or midazolam (MDZ) (all p-values < 0.005) disappearance than all engineered cell lines. HuH-7 had less 1-OH MDZ (all p-values < 0.0005) or 4-OH (all p-values < 0.005) production in metabolism assays than all bioengineered cell lines. We confirmed CYP3A5 metabolic activity with the CYP3A4 selective inhibitor CYP3CIDE. This is the first report of genomic *CYP3A5* bioengineering in human cell lines with drug metabolism analysis.

DMD Fast Forward. Published on May 22, 2017 as DOI: 10.1124/dmd.117.076307
This article has not been copyedited and formatted. The final version may differ from this version.

Introduction:

About 75% of the oral drugs in the United States are enzymatically metabolized by the cytochrome P450 (CYP) family of enzymes (Guengerich, 2008). The CYPs, and other drug metabolizing enzymes, are polymorphic resulting in large variability in metabolic clearance of drugs. *In vitro* systems to study drug metabolism and genetic variation include: cloned and expressed enzymes, human and animal microsomes from individual or pooled donors, freshly isolated and cultured or cryopreserved hepatocytes. However, primary hepatocytes are not an optimal option because they require harvesting liver, are expensive, are not immortalized and are highly variable from specimen to specimen. To study genetic variants' association with metabolism, a genotyped bank of liver microsomes (He et al., 2006), from individual donors, can be examined but cannot sustainably be engineered to study newly identified genetic variants such as rare variants or those found in minority populations. Also, microsomes are difficult to use to study combinations of genetic variants, especially rare variants or those found in minority populations. Liver microsomes are often from Caucasians limiting their use to understand metabolism in minority populations. Furthermore, since microsomes come from various individuals they are genomically heterogeneous, and from uncontrolled environments, while cell line models are, for the most part, genomically identical except for any specifically altered genetic variant. Thus, we developed genetically modified human liver cell lines that are a sustainable option to investigate the impact of genetic variants on drug metabolism.

Recent reports showed, in rats, that knockout of *CYP2E1* (Wang et al., 2016) or *CYP3A1/2* (Lu et al., 2017) using CRISPR/Cas9 could be used in drug metabolism studies. However, using CRISPR/Cas9 to modify human cell lines to study association of genetic variants with drug metabolism has not been reported. We hypothesized that human liver cell lines can be engineered with CRISPR/Cas9 (Mali et al., 2013c; Ran et al., 2013) to evaluate the effect of genetic variants on drug metabolism. Single genetic variants can be engineered into

DMD Fast Forward. Published on May 22, 2017 as DOI: 10.1124/dmd.117.076307
This article has not been copyedited and formatted. The final version may differ from this version.

cell lines that result in altered enzyme activity, gene regulation or protein expression for drug transport or metabolism studies. This paper provides evidence of this concept to study genetic variants in *CYP3A5* and their effect on metabolism of two CYP3A4 and CYP3A5 enzymatic substrates: midazolam (MDZ) a sedative or anesthetic, and tacrolimus (Tac), an immune suppressant. Among the CYP enzymes, CYP3A4 and CYP3A5 are the most abundant in the liver and their expression is highly variable. The *CYP3A5 *3* (rs776746) loss of function allele is highly prevalent in people of Caucasian descent (Roy et al., 2005) (allele frequency = 0.94) and leads to low metabolism rates of Tac (de Jonge et al., 2013) compared with individuals with *CYP3A5 *1* genotype. However, the *CYP3A5 *1* (expresser) allele is enriched in African Americans (AA) (Bains et al., 2013) and leads to rapid metabolism of MDZ, Tac and other drugs. Approximately, 50% of oral drugs are metabolized by CYP3A4 and CYP3A5 (Pelkonen et al., 2008; Tseng et al., 2014). Consequently, the *CYP3A5* genotype is an important factor in determining appropriate doses of drugs. People of African ancestry are often under-dosed initially with Tac following organ transplantation (Jacobson et al., 2011), in part, due to the high prevalence of the *CYP3A5*1* allele in the AA population (allele frequency 0.85). Carriers of the *CYP3A5 *1* allele, often need higher doses of drugs, that are CYP3A5 substrates, to achieve therapeutic drug levels in blood. Therefore there is a need to develop an *in vitro*, cell culture based, system to understand the effects of genetic variants on drug metabolism prior to clinical use of new drugs or to improve dosing of existing drugs.

The first step in development of a suitable liver cell line was to find a clinically relevant parental cell line. To date, there is not a commercially available liver cell line that is diploid at chromosome 7 and expresses *CYP3A5* *1. The Caco-2 cell line (Sambuy et al., 2005) is a human intestinal cell line that metabolizes drugs, but it has five copies of chromosome 7 and thus is not suitable for studying the diploid *CYP3A5* seen in most patients. The HuH-7 cell line (Nakabayashi et al., 1984; Nakabayashi et al., 1985) was derived from a hepatic carcinoma that

DMD Fast Forward. Published on May 22, 2017 as DOI: 10.1124/dmd.117.076307
This article has not been copyedited and formatted. The final version may differ from this version.

can convert the substrate MDZ, primarily through CYP3A4 activity, in cell culture to its metabolite products hydroxylated 1-OH MDZ and 4-OH MDZ (Choi et al., 2009; Sivertsson et al., 2010; Sivertsson et al., 2013). However, HuH-7 cells are not very efficient at MDZ metabolism because they are homozygous for the slow metabolizing *CYP3A5 *3* allele. Thus, there is a need to develop a liver cell line that mimics the rapid drug metabolism associated with the *CYP3A5 *1* genotype in cell culture.

We hypothesized that by genetically modifying the HuH-7 cell line to the more metabolically active *CYP3A5 *1/*1* or *1/*3* genotypes, the cells would have increased MDZ and Tac metabolic activity. To test the hypothesis, we used CRISPR/Cas9 bioengineering (Mali et al., 2013c; Ran et al., 2013) to develop and characterize new cell lines then phenotypically evaluate the genotypes' effects on MDZ and Tac metabolism. These newly engineered cells can be used as a parental cell line in future studies to assess association of additional genetic variants with drug metabolism. This is the first report of genomic *CYP3A5* bioengineering in human cell lines and functional analysis of associated drug metabolism phenotypes.

Materials and Methods:

Selection of HuH-7 hepatocyte cell line as Parental Cell line

We selected HuH-7, liver carcinoma cells from the Japanese Cell Research Bank (cat. number: JCRB0403) because: **A.**) HuH-7 cells metabolized MDZ in cell culture (Sivertsson et al., 2010; Sivertsson et al., 2013). **B.**) HuH-7 cells were diploid, at chromosome 7 where both *CYP3A4* and *CYP3A5* are located; thus, clinically relevant. **C.**) We sequenced the cells at the *CYP3A5 *3*, *6*, and *7* loci and HuH-7 cells carried *3/*3 alleles at the rs776746 locus, a defined variant to change via CRISPR/Cas9 bioengineering to the more functional *1/*1* or *1/*3*

DMD Fast Forward. Published on May 22, 2017 as DOI: 10.1124/dmd.117.076307
This article has not been copyedited and formatted. The final version may differ from this version.

alleles. **D.**) These HuH-7 cells were also **1/*1* at the loss of function *CYP3A4 *22* (rs35599367) allele. **E.**) We confirmed *CYP3A4* and *CYP3A5* mRNA expression by qRT-PCR.

Parental Cell line and Characterization

HuH-7 (Nakabayashi et al., 1984; Nakabayashi et al., 1985), hepatoma cells from a 57 year old Japanese male, were purchased from the Japanese Cell Research Bank and used as parental cell line for genetic modification. Cells were grown in Dulbeco's Modified Eagle Media (DMEM) with high glucose and pyruvate supplemented with 10% Fetal Bovine Serum and Antibiotic-Antimycotic (Gibco). We refer to this as "media" throughout rest of manuscript.

Genotyping of Cell lines

Genomic DNA was isolated from HuH-7 cells using the Roche High-Pure PCR template preparation kit. PCR and sequencing primers (**Supplementary Table 1**), surrounding SNPs *CYP3A4 *22* (rs35599367, C>T), *CYP3A5 *3* (rs776746, 6986A>G), **6* (rs10264272, 14690G>A) and **7* (rs41303343, nonfunctional) were designed using the NCBI primer-BLAST primer design tool. The sequences surrounding the SNPs in the genomic DNA from the HuH-7 cells were PCR amplified using AccuPrime™ Pfx DNA Polymerase kit and then the PCR products were characterized on 1% agarose gel or purified with the Qiagen PCR clean up kit and sequenced. PCR products were then Sanger sequenced using the primers listed in **Supplementary Table 1** by UMGC.

Plasmids, Guide RNA construction and Transfection

DMD Fast Forward. Published on May 22, 2017 as DOI: 10.1124/dmd.117.076307
This article has not been copyedited and formatted. The final version may differ from this version.

A plasmid that expressed a human codon-optimized Cas9 (Mali et al., 2013a; Mali et al., 2013b; Mali et al., 2013c) nuclease was purchased from Addgene. Guide RNAs (gRNAs) targeting the *CYP3A5*3* locus were designed using the CRISPR design tool at http://crispr.mit.edu/. DNA gBLOCKS were designed, synthesized, and purchased from Integrated DNA Technologies combining the gRNA from the CRISPR design tool with the gRNA synthesis protocol(Mali et al., 2013a) from Addgene. The gBLOCKs were TOPO cloned using the Zero Blunt® TOPO® PCR Cloning Kit into pCR™Blunt II-TOPO® vector. Plasmids were expanded in One Shot® *Stbl3*™ Chemically Competent *E. coli* bacteria purchased from Thermo Fisher. Plasmids were sequence verified. Plasmids were then prepared for transfection following the Qiagen Plasmid Maxi Kit. Plasmids were quantified and assessed for purity using a NanoDrop 2000 UV/Vis spectrophotometer. Newly designed gRNAs and hCas9 plasmid DNA were transfected into the HuH-7 cells using a Neon® Transfection System.

Surveyor Assay to select guide RNAs

Genomic DNA was isolated from transfected cells and then we performed Surveyor assay to screen gRNAs for ability to cut at *CYP3A5* *3 locus using a modified protocol(Guschin et al., 2010) along with Surveyor enzyme from Surveyor® Mutation Detection Kit for Standard Gel Electrophoresis from Integrated DNA Technologies. Briefly, DNA was extracted from bulk transfected cells using Roche High-Pure PCR template preparation kit. PCR was performed using AccuPrime™ Taq DNA Polymerase, high fidelity with *CYP3A5* specific primers Cel1F*3 (5'-CAACTGCCCTTGCAGCATTT-3') and Cel1R*3 (5'- ACCCAGGAAGCCAGACTTTG-3') to produce a 397 bp product (if no deletions). Bio-Rad thermocycler was programed as: **1.** 94 °C for 5 minutes, **2.** 94 °C for 15 seconds, **3.** 56°C for 30 seconds, **4.** 68 °C for 0.5 minutes, **5.** Go to step 2, 34 times, **6.** 68 °C for 0.5 minutes, **7.** 4 °C indefinitely. PCR products were denatured

and re-annealed following a published protocol(Guschin et al., 2010) and visualized in a 10% Bio-Rad Criterion™ TBE Polyacrylamide Gel to determine DNA heteroduplexes from heterogeneous cell cultures caused by CRISPR/Cas9 and gRNA targeting (**Supplemental Figure 3**).

Transfection with selected gRNA and hCAS9

To create cell lines that delete the *CYP3A5*3* splice junction, via non-homologous end joining (NHEJ), two selected gRNAs (gRNA1 and gRNA2) and hCas9 plasmids were transfected into the HuH-7 cells using Neon® Transfection System. The two gRNAs target each side of the *CYP3A5**3 locus. The resultant cells were then single cell cloned to produce homogenous cell lines.

To create the single-nucleotide polymorphism (SNP) cell line, gRNA2 was transfected into cells, with homology directed repair (HDR) template. HDR single-stranded DNA template ssODN 3A5*3_E+. The sequence of ssODN 3A5*3_E+ is 5'-gcttaacgaatgctctactgtcatttctaaccataatctctttaaagagctcttttgtctttcaaTATCTCTTCCGTGTTTGGACCACATTACCCTTCATCATATGAAGCCTTGGGTGGCTCC-3'. The underlined a indicates the *3 base that is changed in from a guanine (g). The lower case letters are the intron sequence, while the upper case letters are the exon 3B sequence. The cells were treated with 1 µM SCR7 (Xcessbio) and 5 µM L755,507 (Xcessbio) at the time of transfection and during the 7 days following transfection until single-cell cloning.

Single cell cloning and cell line screening via PCR and DNA Sanger Sequencing

DMD Fast Forward. Published on May 22, 2017 as DOI: 10.1124/dmd.117.076307
This article has not been copyedited and formatted. The final version may differ from this version.

Transfected cells were plated in media/soft agar mixture as previously described (Kim et al., 2014; Dorr et al., 2015), and propagated to become homogenous cell lines. Specifically, in 150 mm^3 15 ml of a 0.6% solution of UltraPure™ Low Melting Point Agarose (Thermo Fisher Scientific, cat. number: 16520-100) in media was plated at 38.5°C and cooled until solid. Next, 15,000 transfected cells in 15 mL of 38.5°C media with 0.3% UltraPure™ Low Melting Point Agarose was layered on top and cooled. The plate was covered with 10 mL media and incubated at 37°C with 5% CO_2 for about 3-5 weeks until cell colonies were visible. Colonies were then picked with a sterile 200 µL pipette tip and transferred to individual wells of a 96-well Collagen I coated plate and cultured until confluent (approximately 3-4 weeks).

For large scale screening, we dissociated the cells using Trypsin-EDTA (0.25%) and transferred half the culture to fresh 96-well plates with media and grown. The remaining cells in the 96-well plate were centrifuged at 350 x g for 5 minutes. Trypsin was removed and the cell pellets were lysed using the QuickExtract™ DNA Extraction Solution from Epicentre. Lysates were used as PCR template and then PCR amplified with an AccuPrime™ Pfx DNA Polymerase kit in 96-well PCR plates. The primers for amplification of the *CYP3A5*3* region were designed using NCBI Primer design (http://www.ncbi.nlm.nih.gov/tools/primer-blast/) and are: 7853F (5'-GCATTTAGTCCTTGTGAGCACTTG-3') and 8303R (5'-CATACGTTCTGTGTGGGGACAAC-3'). Thermocycler was programed as follows: **1.** 94 °C for 5 minutes **2.** 94 °C for 15 seconds **3.** 55 °C for 30 seconds **4.** 68 °C for 30 seconds **5.** Go to step 2, 34 times **6.** 68 °C for 7 minutes **7.** 4 °C indefinitely. PCR products were purified using the MinElute 96 UF PCR Purification Kit (Qiagen), characterized by electrophoresis through a 2% agarose gel and by sequencing of the PCR products. Sequencing was performed by the UMGC using sequencing primer 7884F (5'-ACCTGCCTTCAATTTTTCACTG-3') and 8267R (5'- CTTCACTAGCCCGATTCTGC-3'). Sequence data were analyzed using DNA Star Lasergene and Geneious software.

DMD Fast Forward. Published on May 22, 2017 as DOI: 10.1124/dmd.117.076307
This article has not been copyedited and formatted. The final version may differ from this version.

RNA Splicing Assay

RNA was isolated from the confluent cells using the Qiagen RNeasy Mini Kit. RNA was quantified using the Qubit® 2.0 Fluorometer and the Qubit® RNA BR Assay Kit. RNA was then converted to cDNA using oligo-dT primer and ThermoScript™ Reverse Transcriptase kit. *CYP3A5* *1/*3 or *1/*1 genotyped human liver RNA was also used as controls and cDNA made by same method. PCR primers were developed using the NCBI primer design tool and mRNA sequence file of *CYP3A5* (Genbank accession # BC025176.1) of the 500 base pairs surrounding the *3 nucleotide locus. The cDNA was then used as PCR template with primers: *CYP3A5* cDNA ex2F (5'-GTCACAATCCCTGTGACCTGAT-3') and *CYP3A5* cDNA ex5R (5'-TTGGAGACAGCAATGACCGT-3'). Thermocycler settings were as follows: **1.** 94°C for 5 minutes **2.** 94°C for 15 seconds **3.** 50.5°C for 30 seconds **4.** 68°C for 30 seconds **5.** Go to step 2, 34 times **6.** 68°C for 5 minutes **7.** 4°C forever using the AccuPrime™ Pfx DNA Polymerase kit. PCR products were purified using the QIAquick PCR Purification Kit then characterized by electrophoresis through a 2% agarose gel and imaged using ethidium bromide staining and a Bio-Rad ChemiDoc™ Touch Imaging System.

Quantitative RT-PCR to detect CYP3A5 transcripts

CYP3A5 mRNA was quantified using cells from the MDZ and Tac assays. The primers were the same as for the mRNA splicing assay (**Supplementary Table 1**). . The RNA was the same as the RNA splicing assays and GAPDH primers were used as the reference control. 2 µg of RNA was converted to cDNA and 5 µl of 1 in 20 diluted cDNA was used in a 20µl reaction mix for SYBR Green assay based quantitative RT-PCR. We used a Roche lightcycler and made graphs using Graphpad Prism software.

DMD Fast Forward. Published on May 22, 2017 as DOI: 10.1124/dmd.117.076307
This article has not been copyedited and formatted. The final version may differ from this version.

Immunoblot Analysis for CYP3A5 *1 and *3 variants in engineered cell lines

CYP3A4 and CYP3A5 protein expression was determined by immunoblot analysis. Total lysates were recovered from HuH-7 cells and the new derivative cell lines. For microsome preparation, cells were centrifuged at 1500 rpm for 5 minutes and washed immediately in 1x PBS. This was followed by homogenization using a glass-Teflon homogenizer and a microsome storage buffer (MSB) containing 100 mM potassium phosphate, pH 7.4, 1.0 mM EDTA 20% glycerol with protease inhibitor cocktail. Following differential centrifugation (12,000 × g for 30 minutes; 34,000 × g for 120 minutes), the pellet was resuspended in MSB.

Protein was estimated by using the Bio-Rad protein assay for microsomes and Pierce™ BCA Protein Assay Kit assay for lysates with bovine serum albumin as the standard. 60 µg and 40 µg of total lysate and microsomes, respectively, were separated on 10% sodium dodecyl sulfate-polyacrylamide gel electrophoresis (SDS-PAGE) and immunoblotted with 1:10000 dilution of monoclonal anti-CYP3A4 K03 (Schuetz et al., 1996), or 1:250 dilution of WB-3A5 (Corning, Corning, NY), followed by 1:10000 dilution of secondary antibodies HRP-conjugated anti-mouse and anti-rabbit (Jackson ImmunoResearch Inc., West Grove, PA), respectively. β-Actin protein expression was determined by monoclonal anti-actin (Sigma, St. louis, MO), followed by 1:10000 dilution of secondary antibodies HRP-conjugated anti-mouse. The blot was developed with the ECL™ Western Blotting Reagents (GE Healthcare). Bands on film were optically scanned (Epson).

Midazolam and Tacrolimus Metabolism Assays

HuH-7 and engineered cells were grown to confluence in 12 well Corning™ BioCoat™ Collagen I Multi-well Plates for 3-4 weeks in media. Media was refreshed 2-3 times a week. Cells were then overlaid with Corning Matrigel® Matrix and then induced for 3 days by addition

DMD Fast Forward. Published on May 22, 2017 as DOI: 10.1124/dmd.117.076307
This article has not been copyedited and formatted. The final version may differ from this version.

of 100 µM phenytoin Sodium (USP), diluted in methanol, and 10 µM rifampicin (Sigma), diluted in methanol, in cell culture. Media was changed daily with inducers rifampicin and phenytoin added. On the fourth day, 500 µl of media was added to the cells with 100 µM phenytoin and 10 µM rifampicin with either equal volumes of methanol, as a negative control, or midazolam (MDZ) from Cerriliant diluted in methanol so that MDZ final concentration was 5 µM (1628 ng/mL) in cell culture media. Cells were incubated overnight, and media was collected and assayed for MDZ, 1-OH MDZ and 4-OH MDZ by high performance liquid chromatography mass spectrometry. To determine the metabolic function of the engineered cell lines on Tac (Toronto Research Chemicals Inc.) the same process except we used 6 well collagen coated plates and 1.5 mL with 13 ng/mL Tac reaction volume.

Detection methods for Tac, MDZ, 1-OH MDZ, and 4-OH MDZ

Detection and quantification of midazolam, 1-OH midazolam and 4-OH midazolam in cell culture media was performed using a high-performance liquid chromatograph (Agilent 1200 Series, Santa Clara CA) coupled with a TSQ Quantum triple stage quadrupole mass spectrometer (Thermo-Electron, San Jose, CA). Detection and quantification of tacrolimus was performed using chromatographic separation (Agilent 1100 - High Performance Liquid Chromatography Agilent Inc., Santa Clara, CA) and mass spectrometry (API 4000, Sciex Inc., Redwood City, CA). These detailed methods are in the supplemental files.

CYP3CIDE Experiments

CYP3CIDE (Walsky et al., 2012; Tseng et al., 2014) (Sigma-Aldrich) was used as a selective CYP3A4 inhibitor in cell culture and diluted in DMSO. To determine the concentration

DMD Fast Forward. Published on May 22, 2017 as DOI: 10.1124/dmd.117.076307
This article has not been copyedited and formatted. The final version may differ from this version.

of CYP3CIDE to use in cell culture we performed a dose response in Huh-7 and the *CYP3A5 *1/*1* dd cell line between 100 nM and 1 mM in cell culture using MDZ as the substrate. For further analysis, we used 50 µM CYP3CIDE in our experiments with all cell lines. Dose response curves were assessed using Graphpad Prism software.

Statistical Analysis

All comparisons were conducted using t-test for continuous variables.

Results:

Genotyping of single-cell clones following CRISPR/Cas9 bioengineering of CYP3A5

To create *CYP3A5 *1* cells from the HuH-7 cells that were *CYP3A*3* we altered *CYP3A5* based on CRISPR proto-spacer adjacent motifs (PAM) near the exon 3B splice junction (**Figure 1**). To identify the cell line that had the exon 3B 5' splice junction deleted, we screened single-cell clones by PCR amplifying, then forward and reverse Sanger sequencing of a 451 base pair (bp) region flanking the splice junction (**Figure 1**). The splice junction contains the **3* locus (rs776746) and we deleted this junction to express *CYP3A5 *1* mRNA via alternative splicing. These cells were transfected with gRNA1, gRNA2, and hCas9 plasmids (**Figure 2**). We screened 235 single cell clones and 74 (32%) were mutated. Mutations in modified cell lines were as follows: 22 (9.4%) had a heterozygous frameshift near one of the two gRNA cut sites, 23 (9.8%) were heterozygous for the 77 base pair deletion between gRNA sites, 15 (6.4%) cell lines were homozygous for the 77 base pair deletion, and 14 (6.0%) cell lines were classified as "other". The "other" mutations in cell lines include cell lines that had multiple frameshifts, or were heterozygous for a deletion and frameshift or had other mutations. The heterozygous deletion

DMD Fast Forward. Published on May 22, 2017 as DOI: 10.1124/dmd.117.076307
This article has not been copyedited and formatted. The final version may differ from this version.

cell line was designated *CYP3A5 *1/*3* sd (sd = single deletion) and the homozygous deletion cell line was designated *CYP3A5 *1/*1* dd (dd = double deletion) (**Figure 3**).

To identify the cell line *CYP3A5 *1/*3* pm (pm = point mutation) (**Figure 3**), we screened 212 single cell clones using DNA sequencing that were transfected with hCAS9, gRNA2 and homology-directed repair (HDR) template (**Figure 2**). We found that 33 (16%) were mutated. Mutation in cell lines were as follows: 23 (11%) had a heterozygous frameshift near the gRNA2 cut site, 2 (0.9%) had homozygous frameshift, 1 (0. 5%) had heterozygous point mutation at *3 locus, 0 (0.0%) had homozygous point mutations at *3 locus, and 8 (4.0%) were classified as other. These other mutants include cell lines that had multiple frameshifts, were heterozygous for a deletion and frameshift or had other mutations.

PCR characterization of genomic DNA in new cell lines

Of the cell lines that were sequenced, select cell lines that were *CYP3A5 *1/*3* or *1/*1* by Sanger sequencing screening were validating by PCR characterization of genomic DNA at the *CYP3A5* *3 locus (**Figure 4A and 4B**). The 77 base pair deletions were characterized by PCR amplification of genomic DNA and visualized by 2% agarose gel electrophoresis (**Figure 4B**). Both heterozygous (C*YP3A5 *1/*3* sd) and homozygous (*CYP3A5 *1/*1* dd) cell lines were developed with the 77 base pair *CYP3A5* exon 3B 5' splice junction deleted. The point mutation heterozygous cell line, *CYP3A5*1/*3* pm, did not have a deletion at the splice junction (**Figure 4B**). These cell lines were then further validated with Sanger sequencing (**Supplemental Figure 1**).

CYP3A5 mRNA splicing assay and sequencing of engineered cells

DMD Fast Forward. Published on May 22, 2017 as DOI: 10.1124/dmd.117.076307
This article has not been copyedited and formatted. The final version may differ from this version.

CYP3A5 mRNA splice variants were evaluated by gel electrophoresis at the **3* locus to ensure the deletion, or point mutation, of the *CYP3A5* exon 3B 5' splice junction changed the cells to express the **1* mRNA instead of the **3* mRNA (**Figure 5A and 5B**). Keuhl et al. have previously shown that the 131 base pair exon 3B was present in the *CYP3A5 *3* mRNA and absent in the **1* mRNA (Kuehl et al., 2001), which was confirmed by Busi and Cresteil (Busi and Cresteil, 2005a; Busi and Cresteil, 2005b). Total mRNA from the cell lines was converted to cDNA then PCR amplified with primers that flanked the *CYP3A5* exon 3B to determine if the exon 3B was absent in the engineered cell lines. RNA from human liver cDNA genotyped as **1/*3* were used as the control (**Figure 5B**). This mRNA splicing assay confirmed the absence of the **3* mRNA in the newly developed cell line *CYP3A5 *1/*1* dd. Additionally, the **1/*3* heterozygote cell lines, CYP3A5*1/*3 sd and CYP3A5*1/*3 pm, expressed both the **1* and the **3* mRNA splice variants as compared to the human liver cDNA controls (**Figure 5B**). To further validate the identity of the *CYP3A5* splice variants in the cell lines we sequenced the *CYP3A5* mRNA via Sanger sequencing of the *CYP3A5* RT-PCR products (**Supplemental Figure 2**). The sequences confirmed that the exon 3B was absent in the *CYP3A5 *1/*1* dd cell line when aligned to a *3 sequence. The *CYP3A5 *1/*3* cell lines *CYP3A5 *1/*3* sd and *CYP3A5 *1/*3* pm sequences became jumbled at exon 3B as is expected when sequencing a heterozygote (**Supplemental Figure 2**). However, sequencing in forward and reverse directions confirmed the *CYP3A5 *1/*3* heterozygote engineered cells expressed both the *CYP3A5 *3* and **1* mRNAs.

*Quantitative RT-PCR resulted in elevated CYP3A5 transcripts in *1 expressing cell lines*

Quantitative RT-PCR showed significantly elevated *CYP3A5* mRNA expression in *CYP3A5 *1/*1* dd compared with HuH-7 *CYP3A5 *3/*3* cells (p-value = 2.5×10^{-6}). All

DMD Fast Forward. Published on May 22, 2017 as DOI: 10.1124/dmd.117.076307
This article has not been copyedited and formatted. The final version may differ from this version.

engineered *CYP3A5 *1* cell lines had elevated *CYP3A5* mRNA compared with HuH-7 (p-value $\leq$ 0.0001) (**Figure 5C**). The *CYP3A5 *3* mRNA, expressed in cell lines, was targeted for nonsense-mediated decay[30], as the likley cause of reduced *CYP3A5* mRNA in **3* cell lines. The *CYP3A5 *1/*3* cell lines had intermediate *CYP3A5* mRNA expression compared to HuH-7 *CYP3A5 *3/*3* and *CYP3A5 *1/*1* dd (**Figure 5C**).

Immunoblot confirms for CYP3A5 expression in engineered cell lines

We immunoblotted for the CYP3A5 protein expression in the cell lines using two separate primary antibodies: KO3 (Schuetz et al., 1996), that detects CYP3A family (including CYP3A4 and CYP3A5), or the CYP3A5 specific WB-3A5 (Schmidt et al., 2004) (**Figure 6**). The *CYP3A5*1/*3 sd* cell line visually expressed less CYP3A5 protein expression than *CYP3A5 *1/*1* dd, but higher expression than the *CYP3A5 *3/*3* HuH-7 cells. The *CYP3A5*1/*3* pm cell line had poor CYP3A5 protein expression compared to the *CYP3A5 *1/*3* sd cell line (**Figure 6**). These results were consistent with both the KO3 and WB-3A5 antibodies. It is likely that the K03 antibody did not detect much CYP3A4 protein due to low *CYP3A4* expression in the HuH-7 cell line. Thus, the bioengineered cell lines express CYP3A5 protein.

Metabolism assays show CYP3A5 *1 expressing cells have increased MDZ and Tac metabolism compared with CYP3A5 *3/*3 HuH-7 cells

As shown in **Figure 7A**, we performed an MDZ metabolism assay to determine if the new cell lines metabolized MDZ to the products 1-OH MDZ and 4-OH MDZ. We also quantitated Tac disappearance using the metabolism assay. As expected, the *CYP3A5* *3/*3 (HuH-7) cells had higher levels of Tac (**Figure 7B**) and MDZ (**Figure 7C**) in cell culture after overnight

DMD Fast Forward. Published on May 22, 2017 as DOI: 10.1124/dmd.117.076307
This article has not been copyedited and formatted. The final version may differ from this version.

incubations than *CYP3A5 *1/*3* sd, *CYP3A5 *1/*3* pm or *CYP3A5 *1/*1* dd cell lines because of the decreased metabolism by the *CYP3A5 *3/*3* cells. Furthermore, increased production of 1-OH MDZ (**Figure 7D)** and 4-OH MDZ (**Figure 7E**) was observed by the engineered cell lines compared with the parental HuH-7 cell line. Significant metabolic differences between each of the cell lines were found comparing substrate disappearance or product formation between the engineered cell lines and the HuH-7 parental cell line (all p-values < 0.05) (**Table 1**). Thus, the engineered *CYP3A5 *1* expressing cell lines were more efficient at converting MDZ to its hydroxylated metabolites compared with the *CYP3A5 *3/*3* parental HuH-7 cell line. The engineered *CYP3A5* expressing cells are also more active at metabolizing Tac than the HuH-7 cells which coincides with previous studies with cloned, expressed, *CYP3A4* and *CYP3A5* that demonstrated that the intrinsic clearance of Tac is higher for *CYP3A5* than *CYP3A4 (Dai et al., 2006)*.

CYP3CIDE as a selective CYP3A4 inhibitor in MDZ assays

CYP3CIDE (Walsky et al., 2012; Tseng et al., 2014) is a selective inhibitor of CYP3A4 that can also inhibit CYP3A5 at higher concentrations. The concentration dependent effects of CYP3CIDE are shown in **Figure 8A**. To determine the concentration of CYP3CIDE to use in cell culture we did a dose response study with the HuH-7 (*CYP3A5 *3/*3*) and *CYP3A5 *1/*1* dd cell lines (**Figure 8B**). Following the dose response study, the cell lines were incubated with MDZ with or without 50 µM CYP3CIDE to assess CYP3A5 activity in modified cell lines.

When CYP3CIDE was present, there was slight difference in the MDZ reduction by the HuH-7 cell line ($p = 0.044$). The MDZ reduction was more pronounced in all the *CYP3A5 *1* expressing cell lines comparing with or without CYP3CIDE ($p \leq 0.005$) (**Figure 9A**). The 1-OH MDZ production by HuH-7 cells was lower with CYP3CIDE ($p<0.05$), while all 3 *CYP3A5 *1*

DMD Fast Forward. Published on May 22, 2017 as DOI: 10.1124/dmd.117.076307
This article has not been copyedited and formatted. The final version may differ from this version.

expressing cell lines had even more significant reduction of 1-OH MDZ production (all p-values $\leq$ 0.005) (**Figure 9B**). Further analysis of MDZ metabolism by the cell lines with 4-OH MDZ as the minor metabolic product (**Figure 9C**) showed that CYP3CIDE almost completely halted 4-OH MDZ production by HuH-7 cells (p = 0.007). **Figure 9C** also showed HuH-7 and *CYP3A5 *1/*3* sd cell lines had less 4-OH MDZ production with CYP3CIDE ($p \leq 0.01$ and $p \leq 0.05$, respectively). Neither *CYP3A5 *1/*1* dd nor *CYP3A5 *1/*3* pm had significant 4-OH MDZ production differences with CYP3CIDE (p > 0.05). These CYP3CIDE experiments showed that these cell lines had differential activity when a selective CYP3A4 inhibitor was present; indicating phenotypically active *CYP3A5* which was not present in the parental HuH-7 (*CYP3A5 *3/*3*) cell line.

Discussion:

This study showed the successful CRISPR/Cas9 bioengineering of a human liver cell line, HuH-7, to create new cell lines that express the common *CYP3A5 *1* variant that is known to be highly relevant towards drug metabolism. Unlike recent reports using CRISPR/Cas9 to knock out *CYP2E1* (Wang et al., 2016) or *CYP3A1/2* (Lu et al., 2017) function in rats, we used CRISPR/Cas9 to activate *CYP3A5* expression in human cells lines by conversion of *3* to *1* genotype. This is the first report of engineered cell lines for both heterozygous and homozygous *CYP3A5 *1* expression in human liver cell culture and phenotypic analysis.

This study showed it is possible to use two methods of CRISPR/Cas9 biotechnology to modify the HuH-7 cells to express *CYP3A5 *1* by splice junction deletion using two gRNAs or with one gRNA and a homology directed repair template. Without the need for fluorescent activated cell sorting or less precise limiting dilution techniques, a soft agar clonal selection with expansion on collagen I coated plates technique was used to isolate unique human hepatocyte

DMD Fast Forward. Published on May 22, 2017 as DOI: 10.1124/dmd.117.076307
This article has not been copyedited and formatted. The final version may differ from this version.

cell lines. This technique is important in isolating hepatocyte cell lines because the cells do not grow well as single cells on standard plastic cell culture dishes. Also, growing the cell lines at confluence for 2-3 weeks, layering with Matrigel® and inducing the cells with rifampin and phenytoin increased the hepatocytes metabolic activity. We determined the impact of induction while developing the MDZ metabolism assay. Since induction increased MDZ metabolism in the HuH-7 cells, we did not change the protocol for the genetically modified cell lines or when using Tac as the substrate. In a previous study, 1-OH MDZ production by HuH-7 cells was low, ~2.5 picomol/mg protein/min with rifampicin induction and lower at ~1 picomol/mg protein/min without induction (Sivertsson et al., 2010). In comparison, our induction method in HuH-7 parental cell line produced ~67 ng/mL 1-OH MDZ in media. Although these units are not the same, our method does have higher MDZ metabolism. In our genetically modified cell lines such as, *CYP3A5 *1/*1* dd, 833 ng/ml 1-OH MDZ was formed. Relative to the unmodified HuH-7 (*CYP3A5 *3/*3*) cells, these new cell lines express elevated *CYP3A5* mRNA and led to significantly higher metabolism of Tac and MDZ which are well-known substrates for CYP3A5. The genetically modified cells also produce the expected MDZ metabolites (1-OH MDZ and 4-OH MDZ). Thus, these cells show promise as cell lines for drug metabolism assessment. Since these cells are diploid at chromosome 7 by karyotype (Ding et al., 2013), and by copy number of the *CYP3A5* locus (Forbes et al., 2015), and these new cells have increased drug metabolism, the cells would be ideal to use as parental cell lines to functionally study other genetic variants. Newly discovered variants can also be genetically engineered into the cells to study combinations of genetic variants.

Differential response to drug therapy is common. These differences are in part due to the presence of genetic variants in CYP enzymes that alter drug metabolism and pharmacokinetics. Ethnic minority populations may carry alternative variants or the same variant as Caucasians but with a different allele frequency (Yasuda et al., 2008). Because ethnic

minority populations are generally underrepresented in clinical trials in the United States, differences in pharmacokinetics and response rates are often not detected until the drug has reached the market (Hamel et al., 2016). Therefore, efficient preclinical methods to study how metabolism may be altered in the presence of alternative alleles would be extremely useful. The cell lines that we developed show the potential of the CRISPR/Cas9 biotechnology in the drug metabolism field. We chose *CYP3A5 *3* and **1* as model alleles to genetically engineer since the effect of these alleles on metabolism is well-established *in vitro* by traditional methods and clinically. Specifically, this technology will allow for the creation of cell lines with varying combinations of common alleles, a platform to study rare alleles and those occurring in populations not represented in clinical trials.

A limitation of this study is that we did not investigate the metabolic activity of the newly developed cell lines in the absence of induction. We know induction increases MDZ metabolism in HuH-7 cells (Sivertsson et al., 2010); thus the induction process is necessary to study robust metabolism in the genetically modified cells. Another limitation of this study is that there are possibly off-target effects of the CRISPR/Cas9 engineering that are common in this type of genetic engineering (Cho et al., 2014). We addressed this by selecting gRNAs with the least amount of potential off targets, using the Massachusetts Institute of Technology CRISPR algorithm, and confirmed with sequencing that the DNA was cut at the desired site surrounding the *CYP3A5*3* locus. Additionally, this study showed that we can produce the *CYP3A5 *1* mRNA in human liver cell lines as seen in human samples from previous studies by Kuehl and colleagues and by Busi and Cresteil (Kuehl et al., 2001; Busi and Cresteil, 2005b). We showed that these cells definitively express *CYP3A5 *1* mRNA, and active CYP3A5 enzyme, as either heterozygous or homozygous compared with control HuH-7 cells. However, the two *CYP3A5 *1/*3* heterozygote cell lines either have a 77 bp splice junction deletion or a point mutation and these cell lines have different *CYP3A5* expression and activity than HuH-7. The *CYP3A5 *1/*1*

DMD Fast Forward. Published on May 22, 2017 as DOI: 10.1124/dmd.117.076307
This article has not been copyedited and formatted. The final version may differ from this version.

dd was vastly more metabolically active than the other cell lines and would be the most useful for comparative studies with the *CYP3A5 *1* genotype.

Future work with these methods and developed cell lines include a number of directions. We envision panels of cell lines developed using genetic modification that can be used to study genetic variants associated with drug metabolism. These panels could include variants of particular metabolism genes, gene families, common variants, or rare variants. Common variants or combinations of common variants could be engineered into cell lines and used in preclinical drug metabolism screens to predict pharmacokinetics. Rare variants could also be engineered into the cell lines. If rare alleles were found to alter metabolism it may predict subjects at risk for drug failure or toxicity. It may also allow for early testing of alternative doses for trial subjects carrying combination of variants or rare alleles. There are substantial challenges in studying rare alleles in human clinical trials due to inadequate sample size; therefore, engineered cells could bring extreme value to drug development. In addition, drugs already on the market could be rapidly screened. Since the new cells in this study express *CYP3A5*, the cells are especially useful to study genetic variants that effect *CYP3A5* expression. Finally, it may also be possible that multiple variants could be engineered into a single cell line which would more closely emulate the specific human populations. This technology can potentially lead to faster preclinical development that can save time and money. As the use of this technology expands, we will be able to more accurately predict substrate metabolism, pharmacokinetics, toxicities and efficacy, especially in minority patients with rare genetic variants.

Acknowledgments:

We thank University of Minnesota Genomics Center for numerous molecular biology services. Ajay Israni and Casey Dorr, along with Minneapolis Medical Research Foundation, have filed a provisional patent with the United State Patent and Trademark Office titled: Genetically Modified Cells for Metabolic Studies. The patent application number is 62/459,749. The cell line *CYP3A5 *1/*3* sd is deposited at American Type Culture Collection (ATCC) patent depository under the name “Human liver cell line; 97 *CYP3A5 *1/*3*” with ATCC® patent deposit designation PTA-123710.

DMD Fast Forward. Published on May 22, 2017 as DOI: 10.1124/dmd.117.076307
This article has not been copyedited and formatted. The final version may differ from this version.

Authorship Contributions:

Participated in research design: Dorr, Remmel, Muthusamy, Moriarity, Wu, Guan, Oetting, Jacobson, Israni

Conducted experiments: Dorr, Muthusamy, Israni, Wu, Fisher, Schuetz, Kazuto

Contributed new reagents or analytic tools: Dorr, Remmel, Muthusamy, Wu, Fisher, Moriarity, Israni

Performed data analysis: Dorr, Muthusamy, Fisher, Kazuto, Wu, Oetting

Wrote or contributed to the writing of the manuscript: Dorr, Remmel, Muthusamy, Fisher, Moriarity, Wu, Guan, Oetting, Jacobson, Israni

References:

Caco2 [Caco2] (ATCC® HTB37™).
COSMIC: Catalogue of somatic mutations in cancer.
Bains RK, Kovacevic M, Plaster CA, Tarekegn A, Bekele E, Bradman NN, and Thomas MG (2013) Molecular diversity and population structure at the Cytochrome P450 3A5 gene in Africa. *BMC Genet* **14:**34.
Busi F and Cresteil T (2005a) CYP3A5 mRNA degradation by nonsense-mediated mRNA decay. *Mol Pharmacol* **68:**808-815.
Busi F and Cresteil T (2005b) Phenotyping-genotyping of alternatively spliced genes in one step: study of CYP3A5*3 polymorphism. *Pharmacogenet Genomics* **15:**433-439.
Cho SW, Kim S, Kim Y, Kweon J, Kim HS, Bae S, and Kim JS (2014) Analysis of off-target effects of CRISPR/Cas-derived RNA-guided endonucleases and nickases. *Genome Res* **24:**132-141.
Choi S, Sainz B, Jr., Corcoran P, Uprichard S, and Jeong H (2009) Characterization of increased drug metabolism activity in dimethyl sulfoxide (DMSO)-treated Huh7 hepatoma cells. *Xenobiotica* **39:**205-217.
Dai Y, Hebert MF, Isoherranen N, Davis CL, Marsh C, Shen DD, and Thummel KE (2006) Effect of CYP3A5 polymorphism on tacrolimus metabolic clearance in vitro. *Drug Metab Dispos* **34:**836-847.
de Jonge H, de Loor H, Verbeke K, Vanrenterghem Y, and Kuypers DR (2013) Impact of CYP3A5 genotype on tacrolimus versus midazolam clearance in renal transplant recipients: new insights in CYP3A5-mediated drug metabolism. *Pharmacogenomics* **14:**1467-1480.
Ding Q, Lee YK, Schaefer EA, Peters DT, Veres A, Kim K, Kuperwasser N, Motola DL, Meissner TB, Hendriks WT, Trevisan M, Gupta RM, Moisan A, Banks E, Friesen M, Schinzel RT, Xia F, Tang A, Xia Y, Figueroa E, Wann A, Ahfeldt T, Daheron L, Zhang F, Rubin LL, Peng LF, Chung RT, Musunuru K, and Cowan CA (2013) A TALEN genome-editing system for generating human stem cell-based disease models. *Cell Stem Cell* **12:**238-251.
Dorr C, Janik C, Weg M, Been RA, Bader J, Kang R, Ng B, Foran L, Landman SR, O'Sullivan MG, Steinbach M, Sarver AL, Silverstein KA, Largaespada DA, and Starr TK (2015) Transposon Mutagenesis Screen Identifies Potential Lung Cancer Drivers and CUL3 as a Tumor Suppressor. *Mol Cancer Res* **13:**1238-1247.
Forbes SA, Beare D, Gunasekaran P, Leung K, Bindal N, Boutselakis H, Ding M, Bamford S, Cole C, Ward S, Kok CY, Jia M, De T, Teague JW, Stratton MR, McDermott U, and Campbell PJ (2015) COSMIC: exploring the world's knowledge of somatic mutations in human cancer. *Nucleic Acids Res* **43:**D805-811.
Guengerich FP (2008) Cytochrome p450 and chemical toxicology. *Chem Res Toxicol* **21:**70-83.
Guschin DY, Waite AJ, Katibah GE, Miller JC, Holmes MC, and Rebar EJ (2010) A rapid and general assay for monitoring endogenous gene modification. *Methods Mol Biol* **649:**247-256.
Hamel LM, Penner LA, Albrecht TL, Heath E, Gwede CK, and Eggly S (2016) Barriers to Clinical Trial Enrollment in Racial and Ethnic Minority Patients With Cancer. *Cancer Control* **23:**327-337.
He N, Xie HG, Collins X, Edeki T, and Yan Z (2006) Effects of individual ginsenosides, ginkgolides and flavonoids on CYP2C19 and CYP2D6 activity in human liver microsomes. *Clin Exp Pharmacol Physiol* **33:**813-815.
Jacobson PA, Oetting WS, Brearley AM, Leduc R, Guan W, Schladt D, Matas AJ, Lamba V, Julian BA, Mannon RB, and Israni A (2011) Novel polymorphisms associated with

tacrolimus trough concentrations: results from a multicenter kidney transplant consortium. *Transplantation* **91:**300-308.

Kim JH, Shin HJ, Ha HL, Park YH, Kwon TH, Jung MR, Moon HB, Cho ES, Son HY, and Yu DY (2014) Methylsulfonylmethane suppresses hepatic tumor development through activation of apoptosis. *World J Hepatol* **6:**98-106.

Kuehl P, Zhang J, Lin Y, Lamba J, Assem M, Schuetz J, Watkins PB, Daly A, Wrighton SA, Hall SD, Maurel P, Relling M, Brimer C, Yasuda K, Venkataramanan R, Strom S, Thummel K, Boguski MS, and Schuetz E (2001) Sequence diversity in CYP3A promoters and characterization of the genetic basis of polymorphic CYP3A5 expression. *Nat Genet* **27:**383-391.

Lu J, Shao Y, Qin X, Liu D, Chen A, Li D, Liu M, and Wang X (2017) CRISPR knockout rat cytochrome P450 3A1/2 model for advancing drug metabolism and pharmacokinetics research. *Sci Rep* **7:**42922.

Mali P, Aach J, Stranges PB, Esvelt KM, Moosburner M, Kosuri S, Yang L, and Church GM (2013a) CAS9 transcriptional activators for target specificity screening and paired nickases for cooperative genome engineering. *Nat Biotechnol* **31:**833-838.

Mali P, Esvelt KM, and Church GM (2013b) Cas9 as a versatile tool for engineering biology. *Nat Methods* **10:**957-963.

Mali P, Yang L, Esvelt KM, Aach J, Guell M, DiCarlo JE, Norville JE, and Church GM (2013c) RNA-guided human genome engineering via Cas9. *Science* **339:**823-826.

Nakabayashi H, Taketa K, Yamane T, Miyazaki M, Miyano K, and Sato J (1984) Phenotypical stability of a human hepatoma cell line, HuH-7, in long-term culture with chemically defined medium. *Gan* **75:**151-158.

Nakabayashi H, Taketa K, Yamane T, Oda M, and Sato J (1985) Hormonal control of alpha-fetoprotein secretion in human hepatoma cell lines proliferating in chemically defined medium. *Cancer Res* **45:**6379-6383.

Pelkonen O, Turpeinen M, Hakkola J, Honkakoski P, Hukkanen J, and Raunio H (2008) Inhibition and induction of human cytochrome P450 enzymes: current status. *Arch Toxicol* **82:**667-715.

Ran FA, Hsu PD, Wright J, Agarwala V, Scott DA, and Zhang F (2013) Genome engineering using the CRISPR-Cas9 system. *Nat Protoc* **8:**2281-2308.

Roy JN, Lajoie J, Zijenah LS, Barama A, Poirier C, Ward BJ, and Roger M (2005) CYP3A5 genetic polymorphisms in different ethnic populations. *Drug Metab Dispos* **33:**884-887.

Sambuy Y, De Angelis I, Ranaldi G, Scarino ML, Stammati A, and Zucco F (2005) The Caco-2 cell line as a model of the intestinal barrier: influence of cell and culture-related factors on Caco-2 cell functional characteristics. *Cell Biol Toxicol* **21:**1-26.

Schmidt R, Baumann F, Knupfer H, Brauckhoff M, Horn LC, Schonfelder M, Kohler U, and Preiss R (2004) CYP3A4, CYP2C9 and CYP2B6 expression and ifosfamide turnover in breast cancer tissue microsomes. *Br J Cancer* **90:**911-916.

Schuetz EG, Schinkel AH, Relling MV, and Schuetz JD (1996) P-glycoprotein: a major determinant of rifampicin-inducible expression of cytochrome P4503A in mice and humans. *Proc Natl Acad Sci U S A* **93:**4001-4005.

Sivertsson L, Edebert I, Palmertz MP, Ingelman-Sundberg M, and Neve EP (2013) Induced CYP3A4 expression in confluent Huh7 hepatoma cells as a result of decreased cell proliferation and subsequent pregnane X receptor activation. *Mol Pharmacol* **83:**659-670.

Sivertsson L, Ek M, Darnell M, Edebert I, Ingelman-Sundberg M, and Neve EP (2010) CYP3A4 catalytic activity is induced in confluent Huh7 hepatoma cells. *Drug Metab Dispos* **38:**995-1002.

Tseng E, Walsky RL, Luzietti RA, Jr., Harris JJ, Kosa RE, Goosen TC, Zientek MA, and Obach RS (2014) Relative contributions of cytochrome CYP3A4 versus CYP3A5 for CYP3A-

cleared drugs assessed in vitro using a CYP3A4-selective inactivator (CYP3cide). *Drug Metab Dispos* **42:**1163-1173.

Walsky RL, Obach RS, Hyland R, Kang P, Zhou S, West M, Geoghegan KF, Helal CJ, Walker GS, Goosen TC, and Zientek MA (2012) Selective mechanism-based inactivation of CYP3A4 by CYP3cide (PF-04981517) and its utility as an in vitro tool for delineating the relative roles of CYP3A4 versus CYP3A5 in the metabolism of drugs. *Drug Metab Dispos* **40:**1686-1697.

Wang X, Tang Y, Lu J, Shao Y, Qin X, Li Y, Wang L, Li D, and Liu M (2016) Characterization of novel cytochrome P450 2E1 knockout rat model generated by CRISPR/Cas9. *Biochem Pharmacol* **105:**80-90.

Yasuda SU, Zhang L, and Huang SM (2008) The role of ethnicity in variability in response to drugs: focus on clinical pharmacology studies. *Clin Pharmacol Ther* **84:**417-423.

Footnote:

This study was funded by a Minneapolis Medical Research Foundation Postdoctoral Career Development Award to Casey Dorr and grant support from United States National Institute for Allergy and Infectious Diseases [AI U19 AI070119] to Ajay Israni.

Figure Legends:

Figure 1: *CYP3A5 *3* locus (rs776746) and guide RNA targeting strategy. Guide RNAs (gRNA) were targeted to proto-space adjacent motifs (PAM) sequences on each side of the *CYP3A5 *3* SNP (gRNA1 or gRNA2 locus). Exon 3B sequence is in capital letters while the upstream intron sequence is in lower case letters. There are 77 base pairs between the gRNA guided Cas9 cut sites.

Figure 2: Workflow for development of *CYP3A5* genetically modified cell lines using CRISPR/Cas9 and clonal selection. The *CYP3A5 *3* splice junction was deleted with gRNA1, gRNA2 and Cas9 or the *CYP3A5 *3* SNP was point mutated using gRNA2 and a homology directed repair (HDR) template to convert the **3* guanine to a **1* adenine. Following transfection, the cells were single cell cloned by plating in soft agar. The single cell clones were transferred to collagen I coated plates until confluent. Cells were then expanded or screened by PCR of the *CYP3A5 *3* locus and sequencing of the PCR products.

Figure 3: *CYP3A5* maps of cell lines used in this study. The cell lines used in this study include HuH-7 (*CYP3A5 *3/*3*), *CYP3A5 *1/*3* sd which has a deletion of **3* splice junction at one allele, *CYP3A5 *1/*1* dd which has a deletion of **3* splice junction at two alleles, and the *CYP3A5 *1/*3* pm which has a guanine to adenine point mutation converting one allele from *3 to **1*.

Figure 4: Characterization of genomic DNA *at CYP3A5 *3* loci in genetically modified cell lines. A.) Map of genomic DNA spanning *CYP3A5* exons 3, 3B and 4. **B.)** Electrophoresis

DMD Fast Forward. Published on May 22, 2017 as DOI: 10.1124/dmd.117.076307
This article has not been copyedited and formatted. The final version may differ from this version.

through 2% agarose gel of PCR products spanning the *CYP3A5 *3* locus (rs776746) of genomic DNA from the cell lines. Data show HuH-7 genomic DNA as the reference. *CYP3A5 *1/*3* sd had two different alleles, one allele being the same as the HuH-7 reference and one allele being 77 base pairs shorter than the reference. The 77 base pair deletion indicated deletion of the Exon 3B splice junction. *CYP3A5 *1/*1* 1dd showed no reference allele and thus deletion of the Exon 3B in both alleles. *CYP3A5 *1/*3* pm has one PCR product the same size as the reference which is expected in a point mutant.

Figure 5: Characterization of *CYP3A5* RNA expression in genetically modified cell lines. **A.)** mRNA map of *CYP3A5* exons 3, 3B and 4. **B.)** mRNA splicing assay showed expression of *CYP3A5 *1* mRNA in modified cell lines. Genotyped human liver from a *CYP3A5 *1/*3* genotyped patient was used as control. **C.)** Quantitative RT-PCR showed expression levels of *CYP3A5* in cell lines relative to *GAPDH*. P-value comparing *CYP3A5* mRNA expression levels between cell lines are from a paired two-sample T-test.

Figure 6: Characterization of *CYP3A5* protein expression in genetically modified cell lines. Immunoblot with primary (1º) antibodies K03 antibody (Schuetz et al., 1996) that recognizes CYP family proteins including CYP3A4 and CY3A5, WB-3A5 (Schmidt et al., 2004) that is specific for CYP3A5 or β-actin as a reference.

Figure 7: Midazolam (MDZ) and Tacrolimus (Tac) metabolism assays confirm that *CYP3A5 *1* expressing cells have increased metabolic activity compared with HuH-7 *CYP3A5 *3/*3* expressing cells. A.) Metabolism assay used in this study. Cells were plated on

DMD Fast Forward. Published on May 22, 2017 as DOI: 10.1124/dmd.117.076307
This article has not been copyedited and formatted. The final version may differ from this version.

collagen I coated plates, and grown at confluence for 2-3 weeks then layered with Matrigel®. Cells were then induced with rifampicin and phenytoin for 3 days then substrate of Tac or MDZ was added over night. Cell culture media was collected and assayed for Tac, MDZ or the MDZ products 1-OH MDZ or 4-OH MDZ by liquid chromatography-mass spectrometry. **B.)** Tac was used as the substrate and was assayed to assess its disappearance. Each column represents 5 biological replicates of a representative experiment and shows the disappearance of the Tac caused by the cells' metabolism. **C.)** MDZ was used as the substrate to assess its metabolism. Each column represents 6 biological replicates of a representative experiment and shows the disappearance of the MDZ caused by the cells' metabolism. **D.)** The corresponding 1-OH MDZ products from the MDZ experiments are shown and the **E.)** corresponding 4-OH MDZ products.

Figure 8: CYP3CIDE selective inhibition of CYP3A4 and CYP3A5 and dose response in cell lines A.) CYP3CIDE inhibition of CYP3A4 and CYP3A5 enzymatic activity. CYP3CIDE has a higher affinity on CYP3A4 inhibition than CYP3A5 inhibition. The substrate in this experiment was MDZ and the products of the reactions were 1-OH MDZ and 4-OH MDZ. **B.)** CYP3CIDE dose response curve in HuH-7 (*CYP3A5 *3/*3*) and *CYP3A5 *1/*1* dd cell lines with the 1-OH MDZ product as metabolite. The concentration of 50 µM CYP3CIDE was chosen for further study in other cell lines.

Figure 9: Effect of CYP3CIDE on midazolam metabolism in *CYP3A5* genetically modified cells. Cells were treated with (grey bars) or without 50 µM CYP3CIDE (black bars) and assayed for MDZ metabolism. Each column in **C-E** represents 6 biological replicates of a representative experiment. **C.)** MDZ disappearance by cell lines after incubation of MDZ in presence of CYP3CIDE. **D.)** Production of 1-OH MDZ by cell lines in the presence of CYP3CIDE. **E.)**

DMD Fast Forward. Published on May 22, 2017 as DOI: 10.1124/dmd.117.076307
This article has not been copyedited and formatted. The final version may differ from this version.

Production of 4-OH MDZ by cell lines in the presence of CYP3CIDE. P-values in **C-E** were calculated based on the paired two-sample T-test comparing with or without CYP3CIDE are: ns = not significant and $P > 0.05$, * $P \leq 0.05$, **$P \leq 0.01$, ***$P \leq 0.001$.

DMD Fast Forward. Published on May 22, 2017 as DOI: 10.1124/dmd.117.076307
This article has not been copyedited and formatted. The final version may differ from this version.

Table 1: P-Values Comparing Tacrolimus or Midazolam Metabolic activity between cell lines. P-values were calculated based on the paired two-sample T-test comparing between each cell line. Substrates and Products were quantified by liquid chromatography of the media from the cell cultures.

Cell lines Compared	P-Values			
	Substrates		Products	
	Tac	MDZ	1-OH MDZ	4-OH MDZ
$^{+}$HuH-7 **3/*3* vs. $^{++}$*CYP3A5 *1/*3* sd	5.4×10^{-3}	2.4×10^{-5}	2.3×10^{-6}	7.3×10^{-4}
HuH-7 **3/*3* vs. $^{+++}$*CYP3A5 *1/*1* dd	2.7×10^{-3}	5.3×10^{-4}	8.6×10^{-5}	2.7×10^{-4}
HuH-7 **3/*3* vs. $^{++++}$*CYP3A5 *1/*3* pm	2.7×10^{-2}	5.0×10^{-7}	3.8×10^{-8}	1.3×10^{-3}
*CYP3A5 *1/*3* sd vs. *CYP3A5 *1/*1* dd	1.0×10^{-2}	3.6×10^{-1}	3.5×10^{-2}	1.6×10^{-2}
*CYP3A5 *1/*3* sd vs. *CYP3A5 *1/*3* pm	5.3×10^{-2}	5.3×10^{-1}	1.8×10^{-3}	9.4×10^{-1}
*CYP3A5 *1/*1* dd vs. *CYP3A5 *1/*3* pm	3.1×10^{-2}	4.1×10^{-1}	2.0×10^{-3}	2.4×10^{-2}

DMD Fast Forward. Published on May 22, 2017 as DOI: 10.1124/dmd.117.076307
This article has not been copyedited and formatted. The final version may differ from this version.

*[+]HuH-7 was the parental cell line with CYP3A5 *3/*3 alleles*

*[++]CYP3A5 *1/*3 sd was a bioengineered cell line with the CYP3A5 *1 allele made by deletion of a splice acceptor on one of the alleles.*

*[+++]CYP3A5 *1/*1 dd was a bioengineered cell line with both CYP3A5 *1 alleles made by deletion of a splice acceptor on two of the alleles.*

*[++++]CYP3A5 *1/*3 pm was a bioengineered cell line with the CYP3A5 *1 allele made by a point mutation of a splice acceptor on one of the alleles.*

DMD Fast Forward. Published on May 22, 2017 as DOI: 10.1124/dmd.117.076307
This article has not been copyedited and formatted. The final version may differ from this version.

Figure 1.

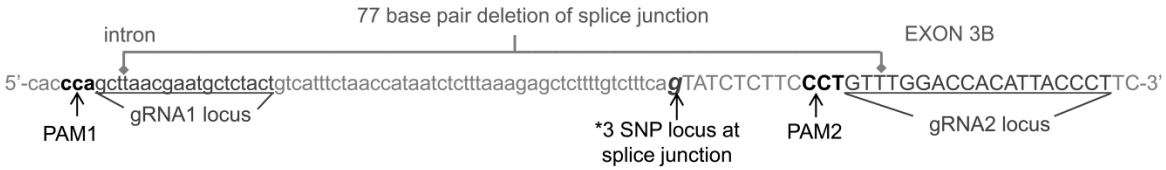

Figure 1

DMD Fast Forward. Published on May 22, 2017 as DOI: 10.1124/dmd.117.076307
This article has not been copyedited and formatted. The final version may differ from this version.

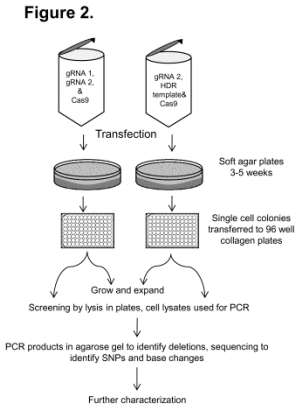

Figure 2

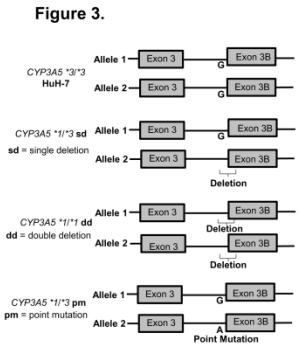

Figure 3

DMD Fast Forward. Published on May 22, 2017 as DOI: 10.1124/dmd.117.076307
This article has not been copyedited and formatted. The final version may differ from this version.

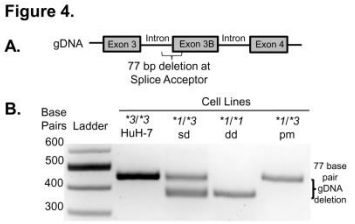

Figure 4

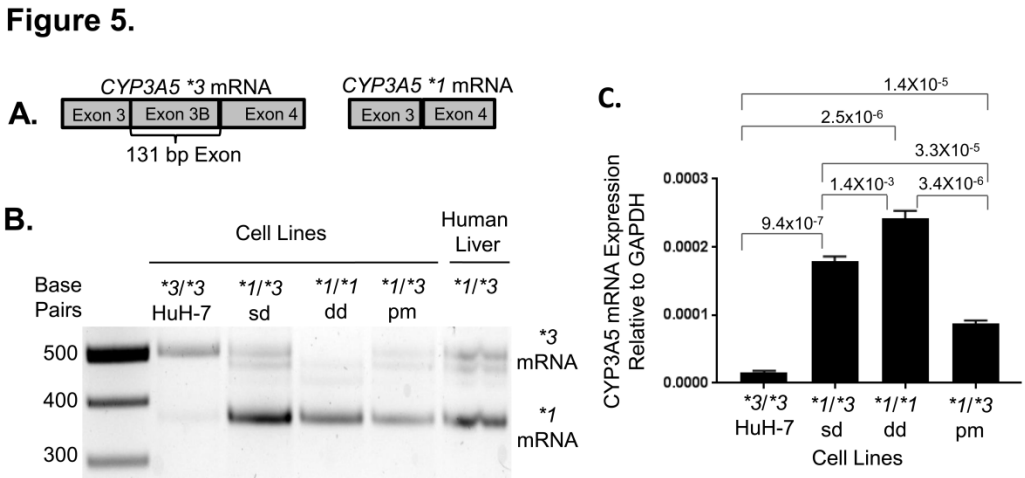

Figure 5

DMD Fast Forward. Published on May 22, 2017 as DOI: 10.1124/dmd.117.076307
This article has not been copyedited and formatted. The final version may differ from this version.

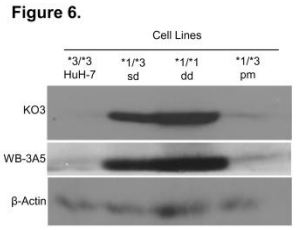

Figure 6

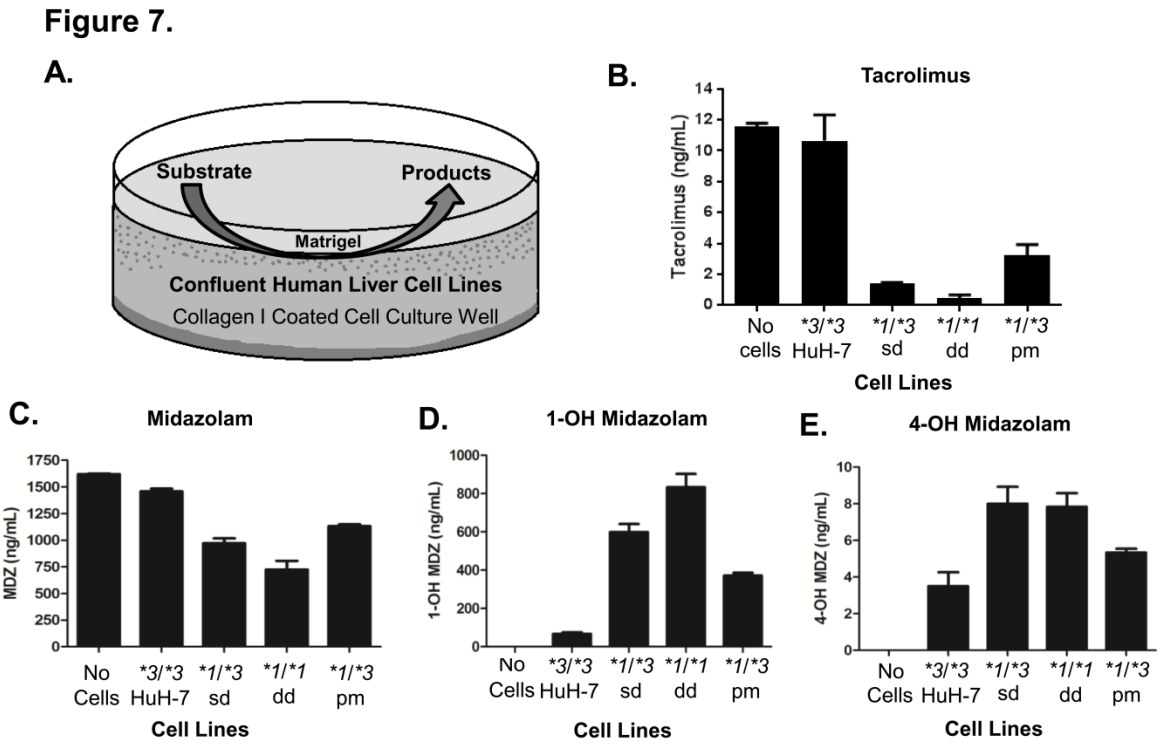

Figure 7

DMD Fast Forward. Published on May 22, 2017 as DOI: 10.1124/dmd.117.076307
This article has not been copyedited and formatted. The final version may differ from this version.

Figure 8.

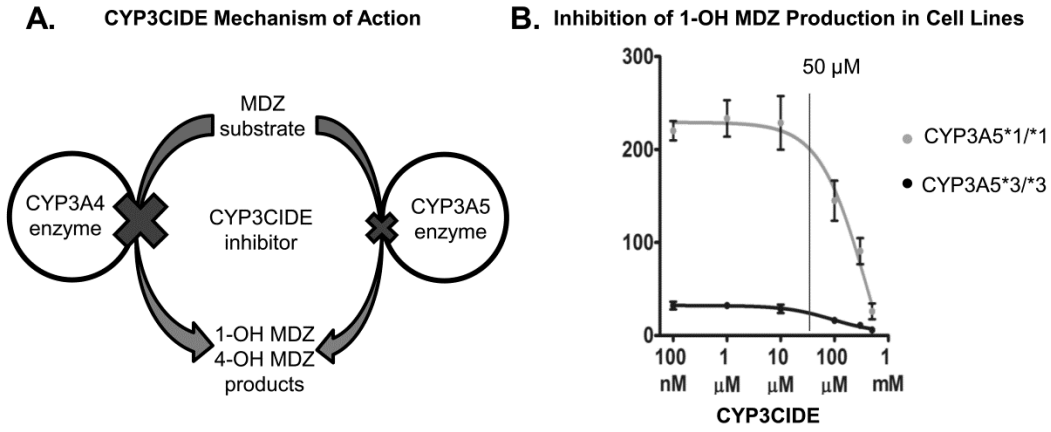

Figure 8

DMD Fast Forward. Published on May 22, 2017 as DOI: 10.1124/dmd.117.076307
This article has not been copyedited and formatted. The final version may differ from this version.

Figure 9.

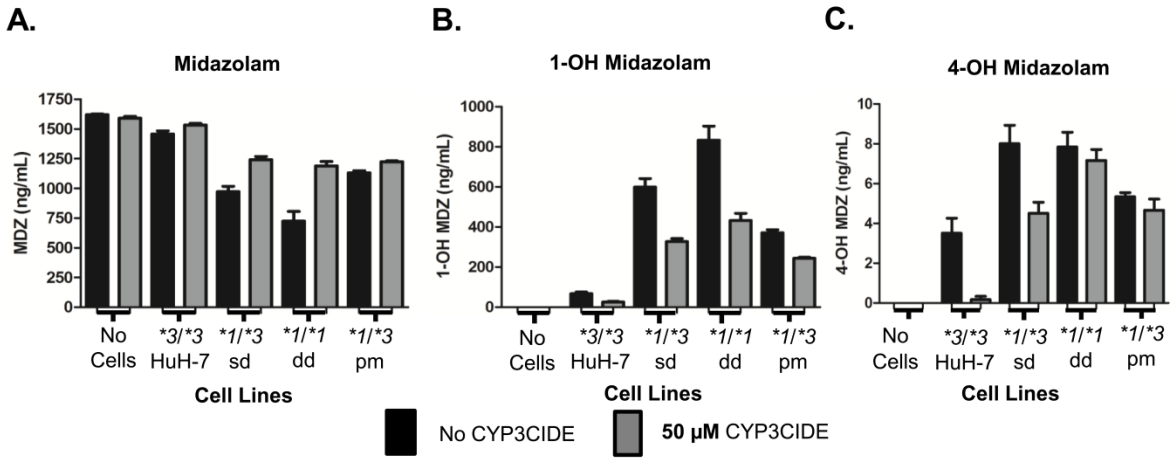

Figure 9

Supplemental Data

Title:

CRISPR/Cas9 genetic modification of *CYP3A5 *3* in HuH-7 human hepatocyte cell line leads to cell lines with increased midazolam and tacrolimus metabolism

Authors:

Casey R. Dorr, Rory P. Remmel, Amutha Muthusamy, James Fisher, Branden Moriarity, Yasuda Kazuto, Baolin Wu, Weihua Guan, Erin Schuetz, William S. Oetting, Pamala A. Jacobson and Ajay K. Israni

Supplemental Figure 1: DNA Sequence Chromatograms of *CYP3A5 *3* locus in Cell Lines
The sequences were aligned to reference sequence from the HuH-7 cell line that had genotype *CYP3A5 *3/*3*. **A.)** Heterozygous deletion of splice junction in cell line *CYP3A5 *1/*3* sd showed jumbled sequence downstream of deletion indicating heterozygosity. **B.)** Homozygous deletion of splice junction in cell line *CYP3A5 *1/*1* dd showed clean sequence downstream of deletion indicating homozygosity. **C.)** Heterozygous point mutation seen in cell line *CYP3A5 1*/*3* pm.

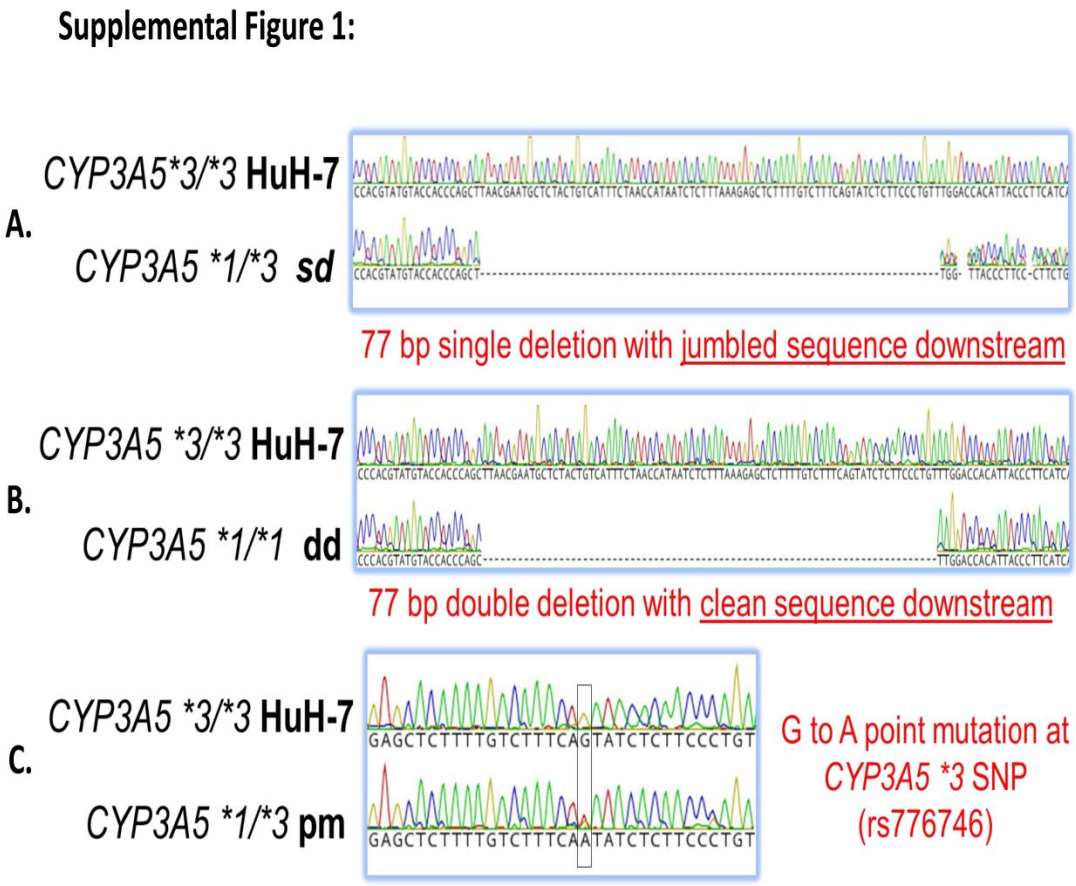

Supplemental Figure 2: Sequence Chromatograms of cDNA from CYP3A5 *3 locus mRNA in Cell Lines. Total RNA was isolated from the cell lines, reverse transcribed with oligo dT primer and the *CYP3A5* mRNA cDNA was sequenced with primers that flank the 131 base pair exon 3B. All cell sequences were aligned to HuH-7 reference control that was *CYP3A5 *3/*3* genotype. **A.)** Absence of exon 3B in cell line *CYP3A5 *1/*3* sd. It is possible we only saw the **1 CYP3A5* in this sequence because previous reports show that *CYP3A5 *3* mRNA is targeted for non-sense mediated decay and would be more difficult to identify in a heterozygote. **B.)** Absence of exon 3B in cell line *CYP3A5 *1/*1* dd. **C.)** Absence of exon 3B in cell line *CYP3A5 1*/*3* pm.

Supplemental Figure 2:

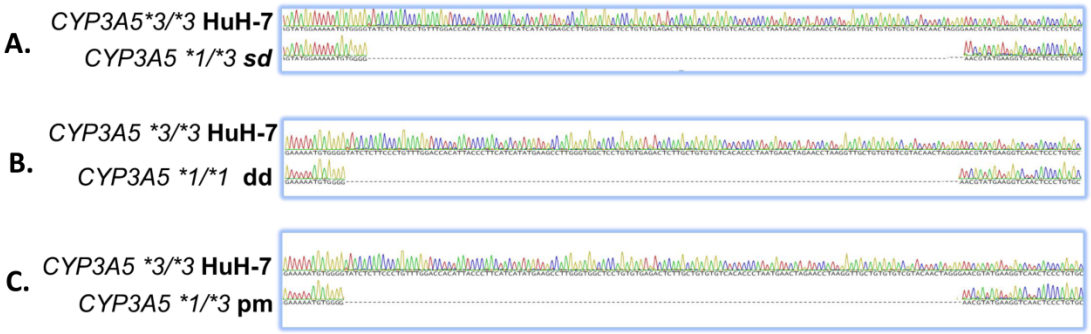

Supplemental Table 1: Primers used in this study for PCR, RT-PCR, and Sequencing.

Gene/Locus	Primer	forward Primer Sequence 5'->3'	Purpose
*CYP3A4 *22*	**22F*	AATTCTGCTGTCAGGGCAAC	PCR Amplification and Sequencing
	**22R*	TTGAGAGAAAGAATGGATCCAAAAA	PCR Amplification and Sequencing
	**22-1F*	GGCATAGAGTCTGCAGTCAGG	Sequencing
	**22-1R*	TCACCTTCTATCACACTCCATCA	Sequencing
	**22-2F*	TCAGTGTCTCCATCACACCC	Sequencing
	**22-2R*	GGATTGTTGAGAGAGTCGATGTT	Sequencing
*CYP3A5 *3*	*8F*	CTGTCAGAGGGGCTAGAGGT	PCR Amplification and Sequencing
	8R	CCTCCCAGGTTCAAGCGATT	PCR Amplification and Sequencing
	7853 F	GCATTTAGTCCTTGTGAGCACTTG	PCR Amplification and Sequencing
	8303 R	CATACGTTCTGTGTGGGGACAAC	PCR Amplification and Sequencing
	7884F	ACCTGCCTTCAATTTTTCACTG	Sequencing
	8267R	CTTCACTAGCCCGATTCTGC	Sequencing
	3A5 ex2F	GTCACAATCCCTGTGACCTGAT	PCR Amplification and Sequencing
	3A5 ex5R	TTGGAGACAGCAATGACCGT	PCR Amplification and Sequencing
	3A5 ex2F Seq	CTGTTTCACTTTGTAGATATGGGAC	Sequencing
	3A5 ex5R Seq	AATCCCACTGGGCCTAAAGAC	Sequencing
*CYP3A5*6*	*4F*	TCTGCCCATCTGTCACCAAT	PCR Amplification and Sequencing
	4R	TTGGCCACATGTCCAGTACT	PCR Amplification and Sequencing
	15488F	GGCACCAGATAACCACCTTC	Sequencing
	15989R	GGGCTCTAGATTGACAAAAACA	Sequencing
*CYP3A5*7*	*12F*	TCCTCCACACATCTCAGTAGGT	PCR Amplification and Sequencing
	12R	TAAGGCCTGACCTTGTCCCT	PCR Amplification and Sequencing
	28064F	ACTTCACGAATACTATGATCATTTACC	Sequencing
	28351R	CATTGACCCTTTGGGAATGA	Sequencing
	28448R	CATTGACCCTTTGGGAATGA	Sequencing
GAPDH	*GAPDHF*	GCATCCTGCACCACCA	qRT-PCR
	GAPDHR	GGATGACCTTGCCCACA	qRT-PCR

Supplemental Figure 3: Surveyor Assay used to select guide RNA. Surveyor nuclease assay indicated HuH-7 parental cells transfected with hCas9, guide RNA 2, and HDR template ssODN successfully mutated the *CYP3A5 *3* locus. Parental and CRISPR modified genomic DNA was used for PCR and surveyor nuclease detection of genome modification at **3* locus. Parental cell PCR products treated with surveyor nuclease had a 397 bp band, while the CRISPR modified cells' PCR products had bands of 397, 236 and 161 bp indicating genetic modification at the **3* locus in bulk transfected cells. These cells were then single-cell cloned to isolate cell line *CYP3A5 *1/*3* pm.

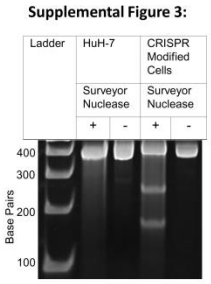

Supplemental Protocols:

Assay - Midazolam and metabolites in cell culture media

Detection and quantification of midazolam, 1-OH midazolam and 4-OH midazolam in cell culture media was performed using a high-performance liquid chromatograph (Agilent 1200 Series, Santa Clara CA) coupled with a TSQ Quantum triple stage quadrupole mass spectrometer (Thermo-Electron, San Jose, CA). The chromatographic separation was performed with a Waters UPLC HSS T3, 2.1 x 50 mm, reversed phase column with a 1.8-micron particle size (Waters, Milford, MA). The mobile phase used for gradient elution consisted of (A) 0.1% formic acid in water, (B) 0.1% formic acid in acetonitrile. The gradient was linear from 20-28% (B) from 0.0- 4.0 min, 20% (B) from 4.25-8.0 min, at a flow rate of 0.3 mL/min, for a total run time of 8.0 minutes. The column temperature was maintained at 45°C. The detector settings of the TSQ Quantum were: ESI with the stainless steel spray needle, positive polarity ionization, selective reaction monitoring mode (SRM); spray voltage, 4500 V; capillary temperature, 400 °C; argon collision gas pressure, 1.5 mTorr; unit resolution for Q1 and Q3, 0.7 u (FWHM).

Analyte Name	Precursor Ion (m/z)	Product Ion (m/z)	Collision Energy (V)	Retention Time (min)
1,4-dihydroxymidazolam	358	290	27	3.04
4-hydroxymidazolam	342	324	2	3.41
1-hydroxymidazolam-d4	346	328	2	4.62
1-hydroxymidazolam	342	324	2	4.69
Midazolam-d4	330	295	8	5.09
Midazolam	326	291	7	5.16

Following the addition of internal standard (120 ng of 1-hydroxymidazolam-d4 and Midazolam-d4) and 5% NH_4OH (0.15 mL), cell culture samples (0.15 mL) were extracted with 1.25 mL of 50:50 Methyl tert-butyl ether:Hexane using a multi-tube vortexer for 10 minutes. Following centrifugation at 15,000 x g for 5 minutes, the supernatant was removed and evaporated to dryness using a nitrogen evaporator (Zymark Turbo Vap LV, Hopkinton, MA) set at 37°C. The residue was reconstituted with 100 µL of mobile phase (A:B, 80:20). Midazolam, metabolites and the deuterated internal standards were obtained from Cerilliant Corporation (Round Rock, Texas). The assay was linear in the range of 1.0 – 1000 ng/mL for midazolam and the metabolites.

Tacrolimus in cell culture media using LC-MS/MS

Sample Extraction

For the calibration standards, an aliquot of 25 uL of each spiking solution is added to 0.50 mL of control blank matrix (cell culture media) in a 13 x 100 mm glass screw-cap culture tube. For the study samples an aliquot of 0.50 mL cell culture media is added to the respective tubes. A 20 uL aliquot of the internal standard (ISTD) working solution (Ascomycin - 1000 ng/mL) is added to each tube and all the samples are vortex-mixed briefly. A volume of 0.50 mL 0.01M ammonium acetate buffer (pH 7.5, adjusted by 1.5% ammonium hydroxide) is added to each sample tube. After a brief mixing, 4 mL of methyl-t-butyl ether is added to extract the desired compounds by mixing for 20 minutes followed by centrifugation for 5 min at 2000 rpm. The aqueous portion is frozen in a freezer at −80 ◦C and the organic portion is transferred to a clean 13 x 100 mm glass culture tube. The organic solvent is evaporated to complete dryness at 37 ◦C under a stream of nitrogen at 15 psi in a Turbo-Vap water bath evaporator. The residue is reconstituted in 0.15 mL of mobile phase. The resulting sample extract is transferred to a glass insert and is placed into an HPLC injection vial and a 7.5uL aliquot of each extracted sample is injected into the LC–MS/MS system.

Chromatographic Separation (Agilent 1100 - High Performance Liquid Chromatography Agilent Inc., Santa Clara, CA) conditions

Chromatographic separation is achieved with an isocratic elution (A: 20, B: 80) using an Acquity UPLC BEH C18, 1.7 um column (2.1 x 50 mm) with mobile phase A: 2 mmole/L ammonium acetate, 0.1% formic acid in DI water and mobile phase B: 2 mmole/L ammonium acetate, 0.1% formic acid in methanol. The flow rate is 0.2 mL/min and the column temperature is set to 65 ◦C. Tacrolimus elutes at 1.23 min (k'=1.23) and ascomycin elutes at 1.19 min (k'=1.16) for a total run time of 4 minutes.

Mass Spectrometer (API 4000, Sciex Inc., Redwood City, CA) conditions

Electrospray ionization (ESI) operating in positive ion mode is used to generate ammonium-adduct ions for mass spectrometric detection. Multiple-reaction mode (MRM) is used to acquire ion counts at different time points. The ESI ion spray voltage is 5000 V and the turbo gas temperature is 400 °C. Nitrogen is used for ion source gas (GS1), ion source gas (GS2), curtain gas (CUR), and collision gas (CAD) and set to flows of 50, 20, 10, and 4 psi, respectively. The declustering potential (DP), collision energy (CE), entrance potential (EP) and collision cell exit potential (CXP) are optimized at instrument settings 95, 30, 10, and 30V respectively. The transitions (precursor to product) monitored are m/z 821.5→ 768.3 for tacrolimus and 809.2→ 756.3 for the internal standard, ascomycin. The dwell time is 50 msec for each transition and both quadruples are maintained at unit resolution.

Calibration Standards

A total of seven standards are used to establish the calibration range (0.125, 0.25, 0.5, 2, 5, 15 and 50 ng/mL).